Chapter 6
Damage Prediction

Material damage in peridynamics (PD) is introduced through elimination of interactions (micropotentials) among the material points. It is assumed that when the stretch, $s_{(k)(j)}$, between two material points, k and j, exceeds its critical value, s_c, the onset of damage occurs. Damage is reflected in the equations of motion by removing the force density vectors between the material points in an irreversible manner. As a result, the load is redistributed among the material points in the body, leading to progressive damage growth in an autonomous fashion.

6.1 Critical Stretch

In order to create a new crack surface, A, all of the micropotentials (interactions) between the material points $\mathbf{x}_{(k^+)}$ and $\mathbf{x}_{(j^-)}$ whose line of action crosses this new surface must be terminated, as sketched in Fig. 6.1. The material points $\mathbf{x}_{(k^+)}$ and $\mathbf{x}_{(j^-)}$ are located above and below the new crack surface, respectively.

The micropotentials for linear elastic deformation can be obtained from Eq. 2.17 as

$$w_{(k^+)(j^-)} = 2\mathbf{t}_{(k^+)(j^-)} \bullet \left(\mathbf{u}_{(j^-)} - \mathbf{u}_{(k^+)}\right), \tag{6.1a}$$

$$w_{(j^-)(k^+)} = 2\mathbf{t}_{(j^-)(k^+)} \bullet \left(\mathbf{u}_{(k^+)} - \mathbf{u}_{(j^-)}\right), \tag{6.1b}$$

or

$$w_{(k^+)(j^-)} = A\left(\left|\mathbf{y}_{(j^-)} - \mathbf{y}_{(k^+)}\right| - \Lambda_{(k^+)(j^-)}\left|\mathbf{x}_{(j^-)} - \mathbf{x}_{(k^+)}\right|\right), \tag{6.2a}$$

$$w_{(j^-)(k^+)} = B\left(\left|\mathbf{y}_{(k^+)} - \mathbf{y}_{(j^-)}\right| - \Lambda_{(j^-)(k^+)}\left|\mathbf{x}_{(k^+)} - \mathbf{x}_{(j^-)}\right|\right), \tag{6.2b}$$

E. Madenci and E. Oterkus, *Peridynamic Theory and Its Applications*,
DOI 10.1007/978-1-4614-8465-3_6, © Springer Science+Business Media New York 2014

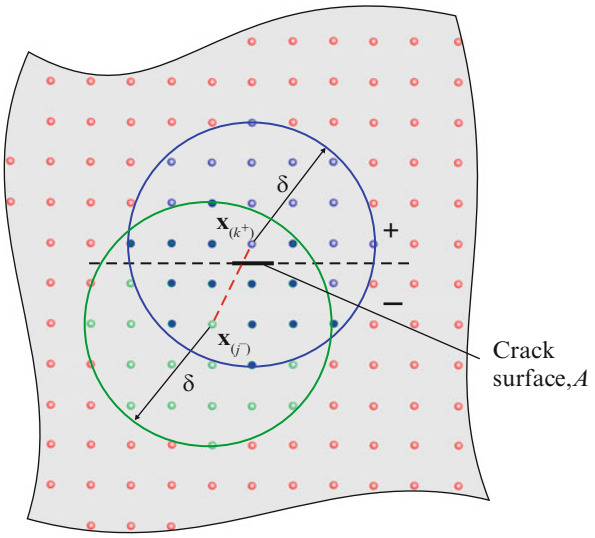

Fig. 6.1 Interaction between material points $\mathbf{x}^+_{(k)}$ and $\mathbf{x}^-_{(j)}$, whose line of action crosses the crack surface

with

$$A = \frac{4ad\delta}{\left|\mathbf{x}_{(j^-)} - \mathbf{x}_{(k^+)}\right|}\Lambda_{(k^+)(j^-)}\theta_{(k^+)} + 4\delta\, bs_{(k^+)(j^-)}, \tag{6.3a}$$

$$B = \frac{4ad\delta}{\left|\mathbf{x}_{(k^+)} - \mathbf{x}_{(j^-)}\right|}\Lambda_{(j^-)(k^+)}\theta_{(j^-)} + 4\delta bs_{(j^-)(k^+)}, \tag{6.3b}$$

in which

$$\theta_{(k^+)} = d\delta \sum_{i=1}^{N} \Lambda_{(k^+)(i)} s_{(k^+)(i)}\, V_{(i)}, \tag{6.4a}$$

$$\theta_{(j^-)} = d\delta \sum_{i=1}^{N} \Lambda_{(j^-)(i)} s_{(j^-)(i)}\, V_{(i)}, \tag{6.4b}$$

and

$$\Lambda_{(k^+)(j^-)} = \frac{\mathbf{y}_{(j^-)} - \mathbf{y}_{(k^+)}}{\left|\mathbf{y}_{(j^-)} - \mathbf{y}_{(k^+)}\right|} \bullet \frac{\mathbf{x}_{(j^-)} - \mathbf{x}_{(k^+)}}{\left|\mathbf{x}_{(j^-)} - \mathbf{x}_{(k^+)}\right|}, \tag{6.5a}$$

$$\Lambda_{(j^-)(k^+)} = \frac{\mathbf{y}_{(k^+)} - \mathbf{y}_{(j^-)}}{\left|\mathbf{y}_{(k^+)} - \mathbf{y}_{(j^-)}\right|} \bullet \frac{\mathbf{x}_{(k^+)} - \mathbf{x}_{(j^-)}}{\left|\mathbf{x}_{(k^+)} - \mathbf{x}_{(j^-)}\right|}. \tag{6.5b}$$

Under the assumption of linear elastic deformation, i.e., $\Lambda_{(j^-)(k^+)} \approx 1$ and $\Lambda_{(k^+)(j^-)} \approx 1$, the expressions for the micropotentials can be rewritten as

$$w_{(k^+)(j^-)} = 4ad^2\delta^2\left(\sum_{i=1}^{N-K^-} s_{(k^+)(i)}s_{(k^+)(j^-)}\,V_{(i)} + \sum_{i=1}^{K^-} s_{(k^+)(i)}s_{(k^+)(j^-)}\,V_{(i)}\right) + 4\delta\, bs^2_{(k^+)(j^-)}\left|\mathbf{x}_{(j^-)} - \mathbf{x}_{(k^+)}\right|, \tag{6.6a}$$

$$w_{(j^-)(k^+)} = 4ad^2\delta^2\left(\sum_{i=1}^{N-J^+} s_{(j^-)(i)}s_{(j^-)(k^+)}\,V_{(i)} + \sum_{i=1}^{J^+} s_{(j^-)(i)}s_{(j^-)(k^+)}\,V_{(i)}\right) + 4\delta bs^2_{(j^-)(k^+)}\left|\mathbf{x}_{(k^+)} - \mathbf{x}_{(j^-)}\right|, \tag{6.6b}$$

in which N represents the total number of material points within the family of $\mathbf{x}_{(k^+)}$ and $\mathbf{x}_{(j^-)}$.

The number of material points within the family of $\mathbf{x}_{(k^+)}$ below the crack surface and intersecting with the crack is denoted by K^-. Similarly, J^+ represents the number of material points above the crack surface within the family of $\mathbf{x}_{(j^-)}$ and intersecting with the crack. Even at the critical stretch, these micropotentials do not completely vanish because of the contribution of the material points to the micropotential through the first term arising from dilatation. Retaining only the interactions crossing the crack surface, the critical values of these micropotentials can be obtained by substituting the critical value, s_c, of the stretch $s_{(k^+)(j^-)}$ and $s_{(j^-)(k^+)}$ as

$$w^c_{(k^+)(j^-)} = \left(4ad^2\delta^2\left(\sum_{i=1}^{K^-} s_c^2\,V_{(i)}\right) + 4\delta\, bs_c^2\left|\mathbf{x}_{(j^-)} - \mathbf{x}_{(k^+)}\right|\right) \tag{6.7a}$$

and

$$w^c_{(j^-)(k^+)} = \left(4ad^2\delta^2\left(\sum_{i=1}^{J^+} s_c^2\,V_{(i)}\right) + 4\delta bs_c^2\left|\mathbf{x}_{(k^+)} - \mathbf{x}_{(j^-)}\right|\right). \tag{6.7b}$$

Hence, the strain energy required to remove the interaction between two material points, $\mathbf{x}_{(k^+)}$ and $\mathbf{x}_{(j^-)}$, can be expressed as

$$W^c_{(k^+)(j^-)} = \frac{1}{2}\,\frac{w^c_{(k^+)(j^-)} + w^c_{(j^-)(k^+)}}{2}V_{(k^+)}V_{(j^-)}. \tag{6.8}$$

Furthermore, the total strain energy required to remove all of the interactions across the newly created crack surface A can be obtained as

$$W^c = \frac{1}{2}\sum_{k=1}^{K^+}\frac{1}{2}\sum_{j=1}^{J^-} w^c_{(k^+)(j^-)} V_{(k^+)} V_{(j^-)} + \frac{1}{2}\sum_{k=1}^{K^+}\frac{1}{2}\sum_{j=1}^{J^-} w^c_{(j^-)(k^+)} V_{(j^-)} V_{(k^+)}, \tag{6.9}$$

for which the line of interaction defined by $|\mathbf{x}_{(k^+)} - \mathbf{x}_{(j^-)}|$ and the crack surface intersect, and K^+ and J^- indicate the number of material points, above and below the crack surface, within the families of $\mathbf{x}_{(k^+)}$ and $\mathbf{x}_{(j^-)}$, respectively. If this line of interaction and crack surface intersect at the crack tip, only half of the critical micropotential is considered in the summation. Substituting for micropotentials given by Eqs. 6.7a, b in Eq. 6.9 results in the critical strain energy required to eliminate all of the interactions across the newly created crack surface A as

$$W^c = s_c^2 \sum_{k=1}^{K^+}\sum_{j=1}^{J^-}\left(2\delta\, b\left|\mathbf{x}_{(j^-)} - \mathbf{x}_{(k^+)}\right| + ad^2\delta^2\left(\sum_{i=1}^{K^-} V_{(i)} + \sum_{i=1}^{J^+} V_{(i)}\right)\right) V_{(k^+)} V_{(j^-)}. \tag{6.10}$$

The total work, W^c, required to eliminate all interactions across this new surface can be equated to the critical energy release rate, G_c, in order to establish the value of critical stretch, s_c, as

$$G_c = \frac{s_c^2 \sum_{k=1}^{K^+}\sum_{j=1}^{J^-}\left(2\delta\, b\left|\mathbf{x}_{(j^-)} - \mathbf{x}_{(k^+)}\right| + ad^2\delta^2\left(\sum_{i=1}^{K^-} V_{(i)} + \sum_{i=1}^{J^+} V_{(i)}\right)\right) V_{(k^+)} V_{(j^-)}}{A}, \tag{6.11}$$

which yields the critical stretch, s_c, expression of

$$s_c = \sqrt{\frac{G_c A}{\sum_{k=1}^{K^+}\sum_{j=1}^{J^-}\left(2\delta\, b\left|\mathbf{x}_{(j^-)} - \mathbf{x}_{(k^+)}\right| + ad^2\delta^2\left(\sum_{i=1}^{K^-} V_{(i)} + \sum_{i=1}^{J^+} V_{(i)}\right)\right) V_{(k^+)} V_{(j^-)}}}. \tag{6.12}$$

Setting $a = 0$ and $4\delta b = c$ reduces this expression to bond-based peridynamics

$$G_c = \frac{1}{2} c s_c^2 \frac{\left\{\sum_{k=1}^{K^+}\sum_{j=1}^{J^-}\left|\mathbf{x}_{(j^-)} - \mathbf{x}_{(k^+)}\right| V_{(k^+)} V_{(j^-)}\right\}}{A}. \tag{6.13}$$

For three-dimensional analysis, the critical energy release rate for bond-based peridynamics was derived by Silling and Askari (2005) in integral form as

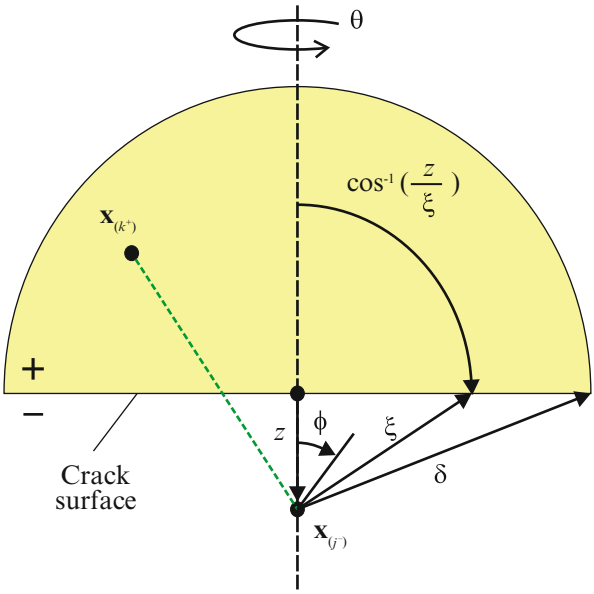

Fig. 6.2 Integration domain of the micropotentials crossing a fracture surface

$$G_c = \int_0^{\delta} \left\{ \int_0^{2\pi} \int_z^{\delta} \int_0^{\cos^{-1} z/\xi} \left(\frac{1}{2} c \xi s_c^2 \xi^2 \right) \sin\phi d\phi d\xi d\theta \right\} dz = \frac{1}{2} c s_c^2 \left(\frac{\delta^5 \pi}{5} \right). \quad (6.14)$$

This integral represents the summation of the work required to terminate all interactions (micropotentials) between point $\mathbf{x}_{(j^-)}$ (below the fracture surface) and all of the points $\mathbf{x}_{(k^+)}$ (above the fracture surface) within its horizon, as shown in Fig. 6.2. The integration in spherical coordinates, (ξ, θ, ϕ), results in the volume of all the points $\mathbf{x}_{(k^+)}$ that are above the fracture surface and within the horizon of point $\mathbf{x}_{(j^-)}$. The line integral includes the contribution of all the points $\mathbf{x}_{(j^-)}$ from 0 to the horizon, δ.

In the case of two-dimensional analysis, the expression for the critical energy release rate for bond-based peridynamics becomes

$$G_c = 2h \int_0^{\delta} \left\{ \int_z^{\delta} \int_0^{\cos^{-1} z/\xi} \left(\frac{1}{2} c \xi s_c^2 \xi \right) d\phi d\xi \right\} dz = \frac{1}{2} c s_c^2 \left(\frac{h\delta^4}{2} \right), \quad (6.15)$$

in which h represents the thickness of the material. The integration is performed in polar coordinates, (ξ, ϕ).

Comparing Eq. 6.13 with Eqs. 6.14 and 6.15 leads to

$$\frac{\sum_{k=1}^{K^+}\sum_{j=1}^{J^-}\left|\mathbf{x}_{(j^-)}-\mathbf{x}_{(k^+)}\right|V_{(k^+)}V_{(j^-)}}{A}=\begin{cases}\dfrac{\delta^5\pi}{5} & \text{three dimensions}\\ \dfrac{h\delta^4}{2} & \text{two dimensions}\end{cases} \tag{6.16}$$

and the second term in Eq. 6.12 can be evaluated as

$$\frac{\left\{\sum_{k=1}^{K^+}\sum_{j=1}^{J^-}\left(\sum_{i=1}^{K^-}V_{(i^-)}+\sum_{i=1}^{J^+}V_{(i^+)}\right)V_{(k^+)}V_{(j^-)}\right\}}{A}=\begin{cases}\dfrac{\delta^7\pi^2}{8} & \text{three dimensions}\\ \dfrac{8h^2\delta^5}{9} & \text{two dimensions}\,.\end{cases} \tag{6.17}$$

Finally, the critical energy release rate can be expressed as

$$G_c=\begin{cases}\left(\dfrac{2\pi}{5}\,b\delta^6+\dfrac{\pi^2}{8}ad^2\delta^9\right)s_c^2 & \text{three dimensions}\\ \left(bh\delta^5+\dfrac{8}{9}ad^2h^2\delta^7\right)s_c^2 & \text{two dimensions}\,.\end{cases} \tag{6.18}$$

After substituting for the peridynamic parameters, a, b, and d, the critical stretch can be expressed as

$$s_c=\begin{cases}\sqrt{\dfrac{G_c}{\left(3\mu+\left(\frac{3}{4}\right)^4\left(\kappa-\frac{5\mu}{3}\right)\right)\delta}} & \text{three dimensions}\\ \sqrt{\dfrac{G_c}{\left(\frac{6}{\pi}\,\mu+\frac{16}{9\pi^2}\left(\kappa-2\mu\right)\right)\delta}} & \text{two dimensions}\,.\end{cases} \tag{6.19}$$

It is worth noting that the critical stretch is a function of the horizon. The value of the horizon brings in the effect of the physical material characteristics, nature of loading, length scale, and the computational cut-off radius. This simple relationship provides the value of critical stretch for a linear elastic brittle material with a known critical energy release rate. If the material exhibits time-dependent nonlinear behavior such as viscoplasticity, a single critical stretch value is not a viable failure criterion. Foster et al. (2011) proposed the use of the critical energy density as a failure criterion in rate-dependent situations. For complex material behavior, there is no simple approach for determining the critical stretch value or critical energy. An inverse approach can be adopted to extract their critical values by performing PD simulations of the fracture experiments with measured failure loads. After each PD simulation with a trial critical value, the PD failure load prediction is compared with that of the measured value, and PD simulations continue with updated critical values until the PD prediction and measured values are within an acceptable range.

6.2 Damage Initiation

In order to include damage initiation in the material response, the force density vector can be modified through a history-dependent scalar-valued function μ (Silling and Bobaru 2005) as

$$\mathbf{t}_{(k)(j)} = 2\delta\left\{ ad\,\frac{\Lambda_{(k)(j)}}{\left|\mathbf{x}_{(j)} - \mathbf{x}_{(k)}\right|}\theta_{(k)} + b\mu\left(\mathbf{x}_{(j)} - \mathbf{x}_{(k)}, t\right)s_{(k)(j)}\right\}\frac{\mathbf{y}_{(j)} - \mathbf{y}_{(k)}}{\left|\mathbf{y}_{(j)} - \mathbf{y}_{(k)}\right|}, \tag{6.20}$$

with the dilatation term

$$\theta_{(k)} = d\delta\sum_{\ell=1}^{N}\Lambda_{(k)(\ell)}\mu\left(\mathbf{x}_{(\ell)} - \mathbf{x}_{(k)}, t\right)s_{(k)(\ell)}V_{(\ell)}, \tag{6.21}$$

where μ can be written as

$$\mu\left(\mathbf{x}_{(j)} - \mathbf{x}_{(k)}, t\right) = \begin{cases} 1 & \text{if} \quad s_{(k)(j)}\left(\mathbf{x}_{(j)} - \mathbf{x}_{(k)}, t'\right) < s_c \quad \text{for all } 0 < t' \\ 0 & \text{otherwise .} \end{cases} \tag{6.22}$$

During the solution process, the displacements of each material point, as well as the stretch, $s_{(k)(j)}$, between pairs of material points, $\mathbf{x}_{(k)}$ and $\mathbf{x}_{(j)}$, are computed and monitored. When the stretch between these material points exceeds its critical stretch, failure occurs; thus, the history-dependent scalar-valued function μ is zero, rendering the associated part of the force density vector to be zero.

6.3 Local Damage

Local damage at a point is defined as the weighted ratio of the number of eliminated interactions to the total number of initial interactions of a material point with its family members. The local damage at a point can be quantified as (Silling and Askari 2005)

$$\varphi(\mathbf{x}, t) = 1 - \frac{\int\limits_H \mu(\mathbf{x}' - \mathbf{x}, t)dV'}{\int\limits_H dV'}. \tag{6.23}$$

The local damage ranges from 0 to 1. When the local damage is one, all the interactions initially associated with the point have been eliminated, while a local damage of zero means that all interactions are intact. The measure of local damage

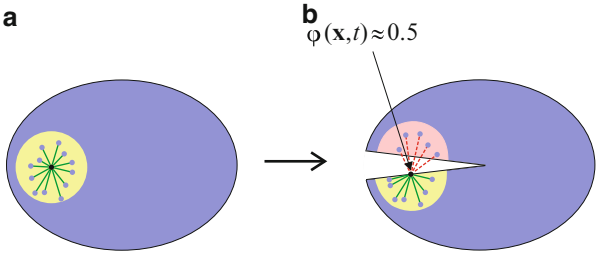

Fig. 6.3 (**a**) All interactions are intact (no damage); (**b**) half of the terminated interactions create a crack

is an indicator of possible crack formation within a body. For example, initially a material point interacts with all materials in its horizon, as shown in Fig. 6.3a; thus, the local damage has a value of zero. However, the creation of a crack terminates half of the interactions within its horizon, resulting in a local damage value of one-half, as shown in Fig. 6.3b.

6.4 Failure Load and Crack Path Prediction

The applicability of the critical stretch as a failure parameter is demonstrated for a linear elastic material by considering the experimental study conducted by Ayatollahi and Aliha (2009). They considered diagonally loaded square plate specimens, shown in Fig. 6.4, to investigate the effect of mode mixity ranging from pure mode I to pure mode II. They provided the failure loads, crack propagation paths for each of the specimens, and fracture toughness of the material, K_{IC}. The edge length of the diagonal square is $2W = 0.15$ m and its thickness is $h = 0.005$ m. The length of the crack is $2a = 0.045$ m, with an orientation angle of α. The material has an elastic modulus of $E = 2940$ MPa, Poisson's ratio of $\nu = 0.38$, and fracture toughness of $K_{IC} = 1.33$ MPa$\sqrt{\text{m}}$. This corresponds to a critical stretch value of 0.089. They also reported the failure loads for varying crack orientation angles of $\alpha = 0^\circ$ (Mode I), 15°, 30°, 45°, and 62.5° (Mode II). The center of the crack coincides with the origin of the Cartesian coordinate system.

The applied load is introduced through a velocity constraint of 10^{-9} m/s along the circular regions in opposite directions. The initial crack is inserted in the PD model by removing the interactions across the crack surface. The force is monitored by summing the forces between the interactions crossing the dotted black line.

As demonstrated in Fig. 6.5, the crack propagation paths obtained from the peridynamic simulations and those of the experimental results agree well with each other for all crack orientation angles. Crack growth initiation angles are also compared between the predictions and measurements. Again a good comparison is obtained, as shown in Fig. 6.6. Finally, the failure loads are compared and it is observed that the failure loads obtained from the peridynamic simulations are within 15 % of the experimental values for all crack inclination angles, as depicted in Fig. 6.7. While the peridynamic simulations closely match the experimental

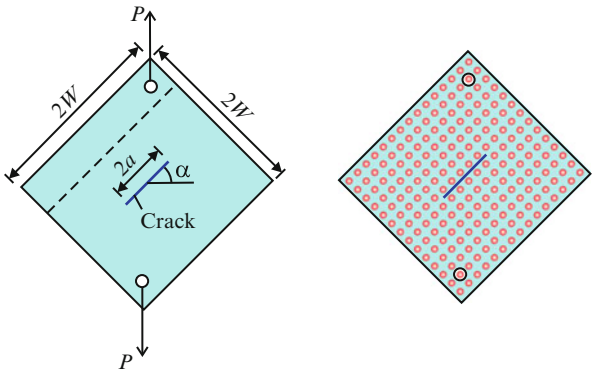

Fig. 6.4 Peridynamic model of the specimen

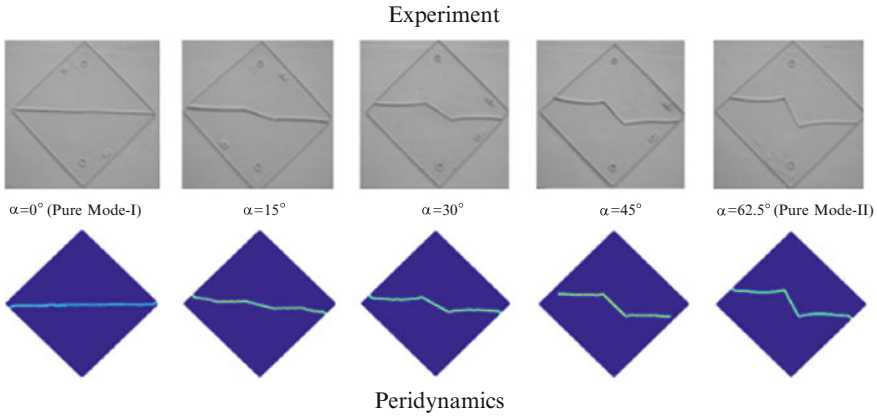

Fig. 6.5 Comparison of experimental and peridynamic crack propagation paths

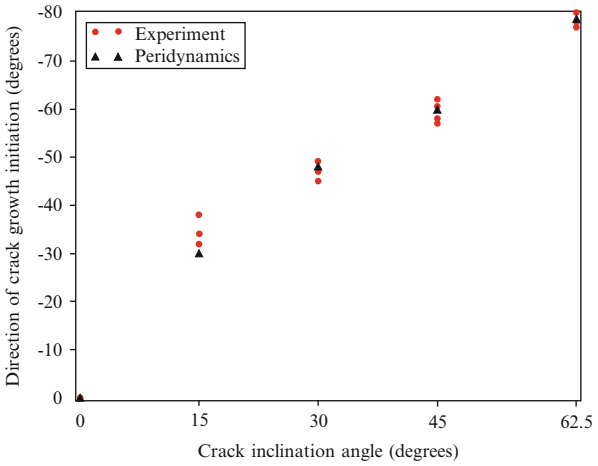

Fig. 6.6 Comparison of crack growth initiation angle between peridynamic and experimental results as a function of crack inclination angle

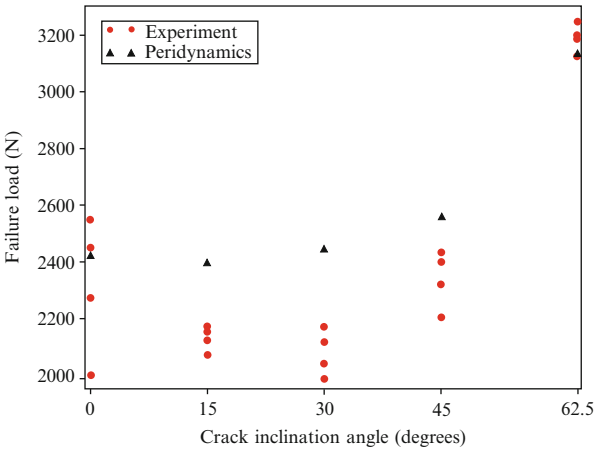

Fig. 6.7 Comparison of the failure load between peridynamic and experimental results as a function of crack inclination angle

results for the pure Mode I and pure Mode II cases, the mixed mode peridynamic failure loads are higher than the experimental values. A possible reason could be due to specimen preparation, which does not ensure a sharp crack tip. The inclined angle of the crack coupled with the shape of the crack tip could in effect change the crack's tip orientation, causing the offset observed in the results. Despite this offset, there exist very good agreement between the peridynamic predictions and those observed in the experiments, which validates the critical stretch values.

References

Ayatollahi MR, Aliha MRM (2009) Analysis of a new specimen for mixed mode fracture tests on brittle materials. Eng Fract Mech 76:1563–1573

Foster JT, Silling SA, Chen W (2011) An energy based failure criterion for use with peridynamic states. Int J Multiscale Comput Eng 9:675–688

Silling SA, Askari E (2005) A meshfree method based on the peridynamic model of solid mechanics. Comput Struct 83:1526–1535

Silling SA, Bobaru F (2005) Peridynamic modeling of membranes and fibers. Int J Non-Linear Mech 40:395–409